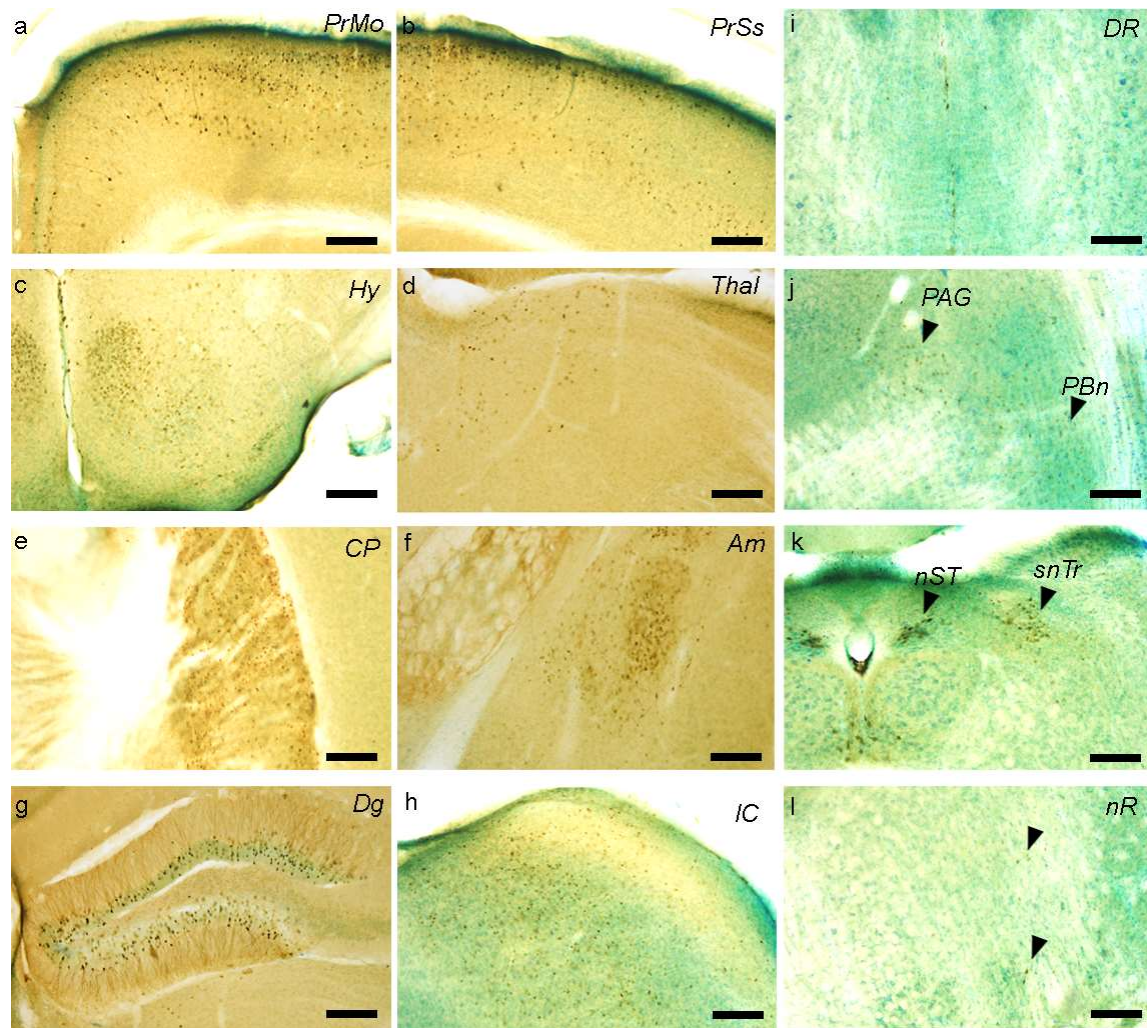


**CRISPR/Cas9-Based Mutagenesis of Histone H3.1 in Spinal Dynorphinergic  
Neurons Attenuates Thermal Sensitivity in Mice**

Mészár et al.

## Supplementary Figure S1

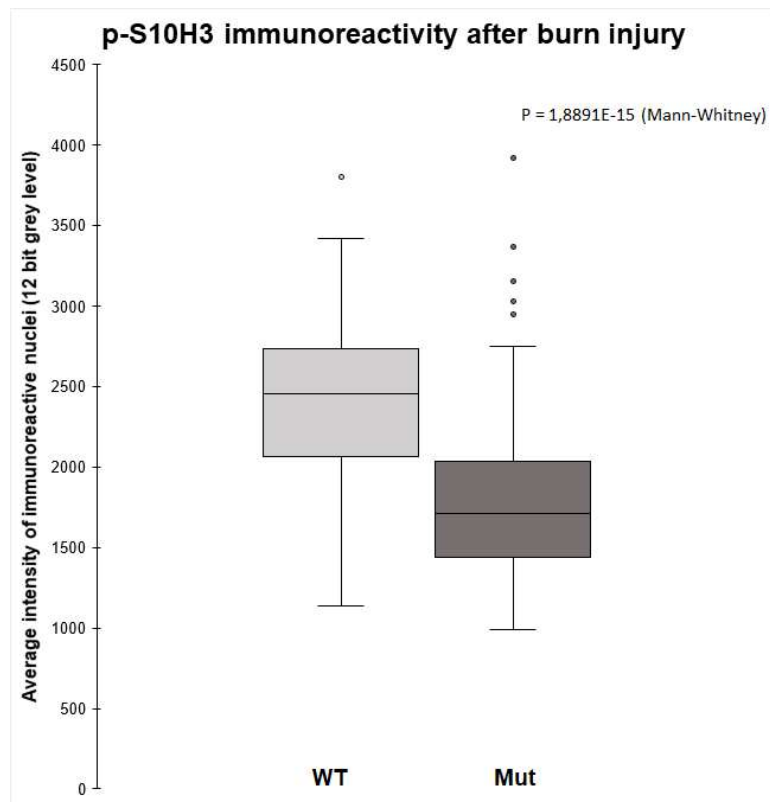


**Conventional immunohistochemistry against EGFP on coronal sections of the whole brain of a Pdyn::cas9-EGFP mouse**

Representative images of the horseradish peroxidase-DiAminoBenzidine conversion of the EGFP signal of Pdyn neurons in coronal sections from a Pdyn::cas9-EGFP hybrid mouse, at the level of the telencephalon/diencephalon, (a-g), midbrain (h-j) and the medulla (k,l). The sections have been counterstained with Toluidine blue to enhance the contrast of the brown cell bodies. *PrMo*, primary motor area; *PrSs*, primary somatosensory area layer 2/3 and layer 5; *Dg*, dentate gyrus; *Thal*, mediiodorsal nucleus of the thalamus; *Hy*, the dorsomedial nucleus of the

hypothalamus; *CP*, caudoputamen; *Am*, central amygdalar nucleus; *IC*, inferior colliculus; *PAG*, periaqueductal gray; *PBn*, parabrachial nucleus; *DR*, dorsal nucleus raphe; *nST*, the nucleus of the solitary tract; *snTr*, the spinal nucleus of the trigeminal nerve; *nR*, reticular nucleus. Scale bars are 200  $\mu\text{m}$ .

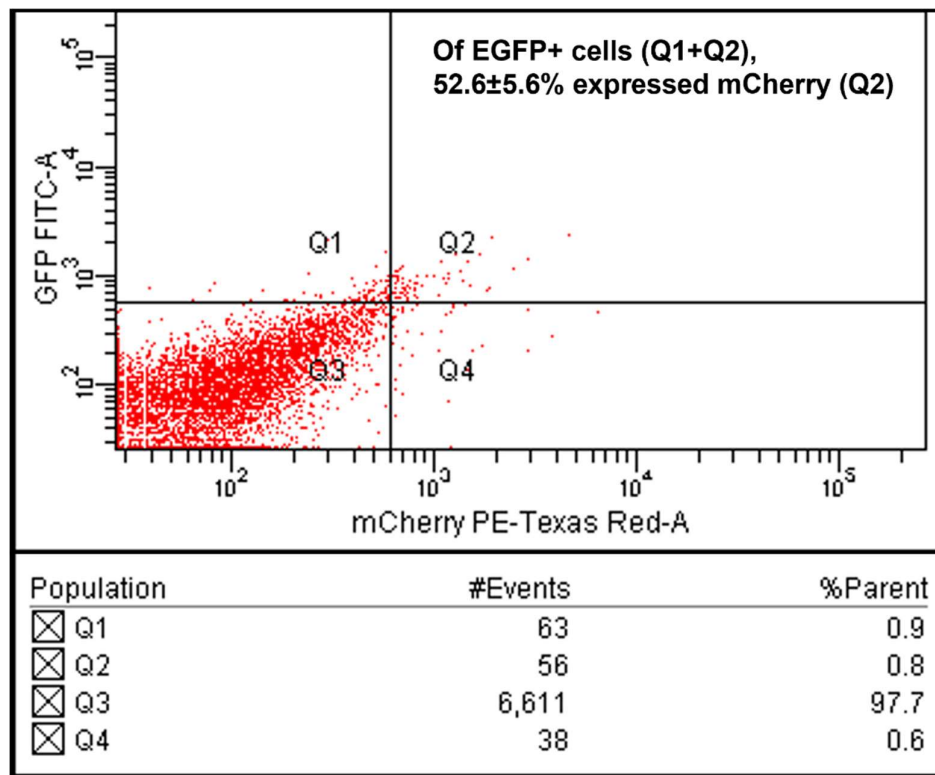
## Supplementary Figure S2



### Evaluation of p-S10H3 immunoreactivity after burn injury

Burn injury-induced p-S10H3 immunoreactivity (IR) was reduced after transduction with AAV9\_mutH3.1 as assessed by intensity profile analysis of p-S10H3-IR nuclei. The box plot indicates the average grey level values of p-S10H3-IR nuclei in spinal cord samples from transduced (AAV9\_mutH3.1; Mut) and non-transduced animals (WT). Y-axis represents the average grey level intensity of p-S10H3-IR nuclei. Dots are outlier values are also indicated in the box plot.

### Supplementary Figure S3

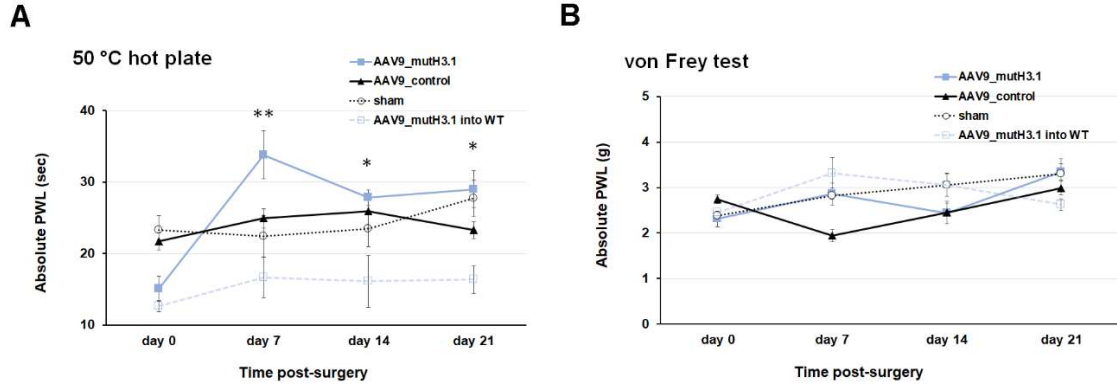


#### FACS gating strategy to quantify double labelled (EGFP+/mCherry+) dynorphinergic neurons in Pdyn::cas9-EGFP mice

Three days after post-infection with AAV9\_mutH3.1, fluorescence-activated cell sorting (FACS) was performed to determine the percentage of EGFP-positive Pdyn neurons in the spinal cord that express mCherry (*i.e.* double tagged neurons).

Scatter plots of green fluorescence intensity on the x-axis (arbitrary units; excitation 488 nm/emission 510/20 nm) and red fluorescence intensity on the y-axis (arbitrary units; excitation 586 nm/emission 610/20 nm) from a representative FACS experiment demonstrates that about half of EGFP-expressing Pdyn neurons were infected by the AAV9\_mutH3.1 based on their mCherry fluorescence.

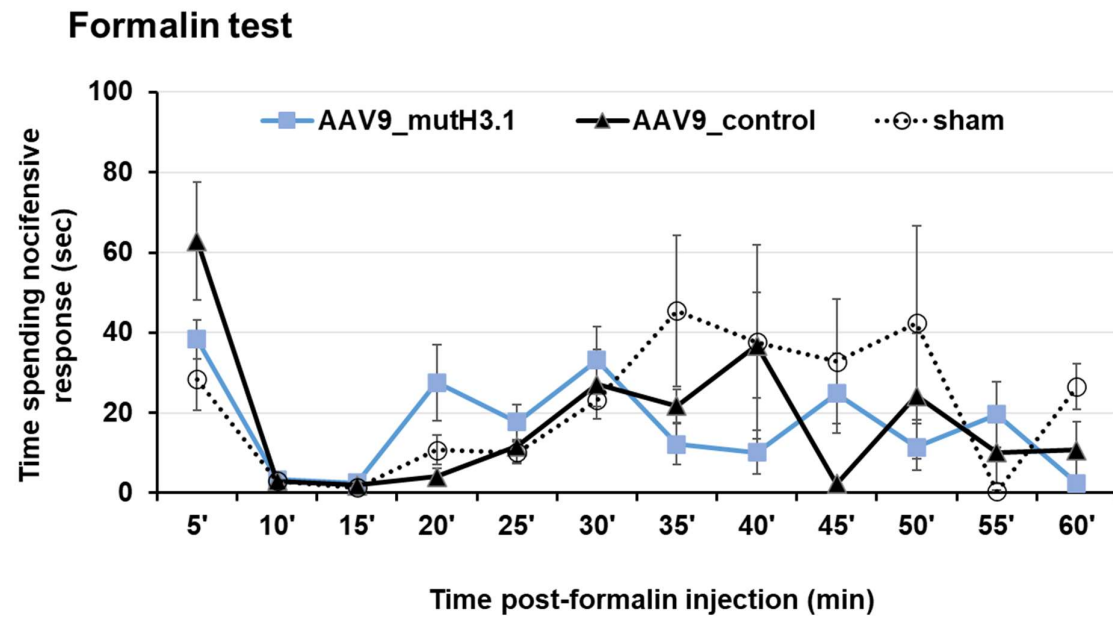
## Supplementary Figure S4



### Absolute values of paw withdrawal latency to thermal- and mechanical pain

Changes in paw withdrawal latencies (PWL) to thermal- (A) and mechanical (B) stimuli were evaluated before (day 0) and after the surgery (day 7, 14, 21) in different groups of Pdyn::cas9-EGFP mice (*i.e.* AAV9\_mutH3.1, AAV9\_control, sham-operated) and also in wild-type animals transduced with AAV9\_mutH3.1. Values at Day 0 represent the pre-surgery baseline values (BTM). (A) \* $p < 0.05$  and \*\* $p < 0.01$  compared with the BTM ( $p = 0.007$  on day 7,  $p = 0.01$  on day 14 and 21, *non-parametric Mann-Whitney U test*). (B) Absolute values of paw withdrawal latency to painful mechanical stimuli showed no significant alterations within, and differences between the groups.

## Supplementary Figure S5



### Assessment of formalin-induced somatic pain

This behavior was quantified as the length of time spent performing a nocifensive response (licking, biting, and shaking) in 5 min periods across an hour after application of formalin. Raw data of the time spent with formalin-induced pain-related movements in each group are presented. There were no statistically significant differences between the groups, at 0.05 level.

See also **Supplementary Table S4** for statistical information.

**Supplementary Table S1. Key Resources**

REAGENT	COMPANY	CATALOG OR STOCK NUMBER / version information / external link
<b>Experimental animals</b>		
Pdyn-IRES-Cre mice	The Jackson Lab. ME, USA	# 027958
Rosa26-LSL-Cas9	The Jackson Lab. ME, USA	# 026175
C57BL/6	AnimaLab Hungary Kft, Hungary	<a href="https://animalab.eu/">https://animalab.eu/</a>
<b>Viral preps</b>		
Custom made- AAV9 mutH3.1.1	SignaGen Labs. MD, USA	# SL100865
pAAV-EF1a-double floxed- hChR2(H134R)-mCherry- WPRE-HGHpA	addgene, MA, USA	Addgene viral prep # 20297-AAV9
<b>Software/device</b>		
sgRNAs designing	broadinstituite.org	<a href="https://portals.broadinstitute.org/gpp/public/analysis-tools">https://portals.broadinstitute.org/gpp/public/analysis-tools</a>
hot/cold plate	Ugo Basile, Italy	#35150
dynamic plantar aesthesiometer	Ugo Basile, Italy	#161
Snapgene 5.1.0	GSL Biotech LLC, CA, USA	<a href="https://www.snapgene.com">https://www.snapgene.com</a>
Olympus FV3000 confocal systems	Olympus, Tokyo, Japan	<a href="https://www.olympus-global.com/">https://www.olympus-global.com/</a>
Neurolucida	MBF BioScience, Williston, Vermont, USA	v11.07
FACS Aria III	BD Biosciences, CA, USA	<a href="https://www.bdbiosciences.com/">https://www.bdbiosciences.com/</a>
FACSDiva 6.1.3	BD Biosciences, CA, USA	<a href="https://www.bdbiosciences.com/">https://www.bdbiosciences.com/</a>
Vibrating blade vibratome	Leica Biosystems, Wetzlar, Germany	VT 1000S
FV31S-DT	Olympus, Tokyo, Japan	<a href="https://www.olympus-global.com/">https://www.olympus-global.com/</a>
Scyscan1272 X-ray High-Resolution Microtomography (micro-CT)	Bruker,Kontich, Belgium	<a href="https://www.bruker.com/en/products-and-solutions/preclinical-imaging/micro-ct/skyscan-1272.html">https://www.bruker.com/en/products-and-solutions/preclinical-imaging/micro-ct/skyscan-1272.html</a>
SkyScan NRecon software (version 2.0.4.2)	Micro Photonics Inc, PA, USA	<a href="https://www.microphotonics.com/products/micro-ct/nrecon-reconstruction-software/">https://www.microphotonics.com/products/micro-ct/nrecon-reconstruction-software/</a>
RadiAnt DICOM Viewer & 3D Volume rendering tool	Medixant, Poznań, Poland	<a href="https://www.radiantviewer.com/">https://www.radiantviewer.com/</a>

OriginPro9	OriginLab Corp., MA, USA	<a href="https://www.originlab.com/">https://www.originlab.com/</a>
Primer3Plus		<a href="https://primer3plus.com/">https://primer3plus.com/</a>
Fiji		<a href="https://imagej.net/software/fiji/">https://imagej.net/software/fiji/</a>
<b>Chemicals and tools</b>		
Alzet osmotic pump	DURECT Corporation, CA, USA	#1003D
5-0 coated vicryl absorbable suture	Ethicon NJ, USA	#J391H
DAB Peroxidase substrate kit	Vector Labs. Inc., CA, USA	#SK-4100
ExtAvidin peroxidase conjugate	Sigma, MI, USA	#E-2886
TRIzol™ Reagent	Thermo Fisher Sci. Inc. MA, USA	#15596026
High-Capacity cDNA Reverse Transcription Kit	Thermo Fisher Sci. Inc. MA, USA	#4368814
RNasin® Ribonuclease Inhibitor	Promega, WI, USA	# N2111
DreamTaq DNA Polymerase	Thermo Fisher Sci. Inc. MA, USA	#EP0701
BenchTop 100 bp DNA ladder	Promega	#G8291
<b>Primary antibodies</b>		
Chicken polyclonal to GFP	abcam, Cambridge, UK	#ab13970
Rat monoclonal [5F8] to Red Fluorescent Proteins (RFP)	Chromotek GmbH, Planegg-Martinsried, Germany	#5f8-100
p-S10H3	abcam Cambridge, UK	#ab5176
Guinea pig Polyclonal ProDynorphin antibody	GeneTex Irvine, CA, USA	# GTX10280
<b>Secondary antibodies</b>		
Goat anti-Rat IgG, Alexa Fluor 555	Thermo Fisher Sci. Inc. MA, USA	#A-21434
Alexa Fluor® 488 AffiniPure Donkey Anti-Chicken IgY	Jackson ImmunoResearch Europe Ltd, Cambridgeshire, UK	#703-545-155
Alexa Fluor® 647 AffiniPure Donkey Anti-Guinea Pig IgG	Jackson ImmunoResearch	#706-605-148

	Europe Ltd, Cambridgeshire, UK	
Biotin-SP-AffiniPure Donkey Anti-Chicken IgY	Jackson ImmunoResearch Europe Ltd, Cambridgeshire, UK	#703-065-155
Neurobasal medium	Thermo Fisher Sci. Inc., MA, USA	#21103049
Glutamax supplement	Sigma, MI, USA	#135050-061
7.5% Na-bicarbonate	Thermo Fisher Sci. Inc., MA, USA	#25080
papain	Merck Life Sci., NJ, USA	#107144
hyaluronidase type I	Merck Life Sci., NJ, USA	#H-3506
Trypsin-EDTA (0.25%), phenol red	Thermo Fisher Sci. Inc., MA, USA	#25200-056
FBS	Sigma, MI, USA	#F9665
Nylon net filter	Millipore, MA, USA	# NY4100010

**Supplementary Table S2****Primer sequences applied in this study**

Name	5'-3' sequence
STOP-cas9 WT_rev <sup>#</sup>	CAG GAC AAC GCC CAC ACA
STOP-cas9 mut_for <sup>#</sup>	TCC CCA TCA AGC TGA TCC
STOP-cas9 mut_rev <sup>#</sup>	CTT CTT CTT TGG GGC CAT CT
STOP-cas9 WT_for <sup>#</sup>	AAG GGA GCT GCA GTG GAG TA
cre_for <sup>\$</sup>	GCA TTA CCG GTC GAT GCA ACG AGT GAT GAG
cre_rev <sup>\$</sup>	GAG TGA ACG AAC CTG GTC GAA ATC AGT GCG
mCherry_for*	GGCGAGGAGGATAACATGG
mCherry_rev*	GATGTTGACGTTGTAGGCGC
GAPDH_for*	ACCCATCACCATCTTCCA
GAPDH_rev*	CATCACGCCACAGCTTCC

<sup>#</sup>Primer set for genotyping Rosa26-LSL-Cas9 line was recommended by The Jackson Laboratory.

<sup>\$</sup>Primer set for genotyping Pdyn<sup>cre</sup> line was recommended by the Mouse Genetics Core (<https://mgc.wustl.edu/>).

\*Primer sets were designed by using Primer3Plus.

**Supplementary Table S3.****sgRNAs sequences targeting wild-type histone H3.1**

Name	Orientation	PAM sequence	sgRNA sequence
sgRNA1	antisense	AGG	TGTCCTCAAACAGACCCACA
sgRNA2	antisense	CGG	GCCGCCGGTGGACTTGCGAG
sgRNA3	antisense	GGG	GGTGGCTAGCTGCTTGCAGC

The input sequence was the *Mus musculus* H3 clustered histone 1 (H3c1; Gene ID: 360198). This gene is intronless and encodes a replication-dependent histone that is a member of the histone H3 family. sgRNAs sequences targeting H3 clustered histone 1 (*i.e.* histone H3.1) was designed with the aid of broadinstitute.org (see **Supplementary Table S1**).

**Supplementary Table S4. Statistical analysis**

Figure	Comparison	Analysis	p/U/χ²/df values	number of animals
Fig4b	The overall influence of the treatment with the AAV9_mutH3.1 on paw withdrawal latency (PWL) in response to noxious heat	Kruskal-Wallis ANOVA	p=0.009 df=3 χ²=11.533	7
Fig4b	The overall influence of the treatment with the AAV9_control on PWL in response to noxious heat	Kruskal-Wallis ANOVA	p=0.487 df=3 χ²=2.433	6
Fig4b	The overall influence of the sham operation on PWL in response to noxious heat	Kruskal-Wallis ANOVA	p=0.460 df=3 χ²=2.580	4
Fig4b	PWL in response to noxious heat of AAV9_mutH3.1-treated vs sham between the corresponding days	Non-parametric Mann-Whitney test	day7: p=0.006 U=27; day14: p=0.012 U=27; day21: p=0.029 U=26	7 AAV9_mutH3.1-treated and 4 sham treated
Fig4b	PWL in response to noxious heat of AAV9_mutH3.1-treated vs AAV9_control between the corresponding days	Non-parametric Mann-Whitney test	day7: p=0.001 U=42; day14: p=0.013 U=38; day21: p=0.001 U=42	7 AAV9_mutH3.1-treated and 6 AAV9_control treated
Fig4c	The overall influence of the treatment with the AAV9_mutH3.1 on PWL in response to mechanical force	Kruskal-Wallis ANOVA	p=0.106 df=3 χ²=6.110	4

Fig4c	The overall influence of the treatment with the control-AAV9 on PWL in response to mechanical force	Kruskal-Wallis ANOVA	p=0.106 df=3 $\chi^2=6.110$	3
Fig4c	The overall influence of the sham operation on PWL in response to mechanical force	Kruskal-Wallis ANOVA	p=0.075 df=3 $\chi^2=6.897$	3
Fig4c	PWL in response to mechanical pain of AAV9_mutH3.1-treated vs sham between the corresponding days	Non-parametric Mann-Whitney test	day7: p=0.4 U=9; day14: p=0.4 U=3; day21: p=0.859 U=7:	4 AAV9_mutH3.1-treated and 3 sham treated
Fig4c	PWL in response to mechanical pain of AAV9_mutH3.1-treated vs AAV9_control treated mice between the corresponding days	Non-parametric Mann-Whitney test	day7: p=0.228 U=10; day14: p=0.857 U=7; day21: p=0.114 U=11	4 AAV9_mutH3.1-treated and 3 AAV9_control treated mice
Fig4d	The overall influence of the treatment with the AAV9_mutH3.1 on the 1 <sup>st</sup> phase of the formalin response	Kruskal-Wallis ANOVA	In the 1 <sup>st</sup> phase: p=0.290 df=2 $\chi^2=2.474$	6 AAV9_mutH3.1 3 AAV9_control and 3 sham
Fig4d	The overall influence of the treatment with the AAV9_mutH3.1 on the 2 <sup>nd</sup> phase of the formalin response	Kruskal-Wallis ANOVA	In the 2 <sup>nd</sup> phase: p=0.148 df=2 $\chi^2=3.807$	6 AAV9_mutH3.1 3 AAV9_control and 3 sham
Fig4d	Integrated time in response to formalin in the groups of AAV9_mutH3.1-	Non-parametric Mann-Whitney test	In the 1 <sup>st</sup> phase: p=1 U=9  In the 2 <sup>nd</sup> phase:	6 AAV9_mutH3.1 treated and 3 AAV9_control treated mice

	treated <i>vs</i> AAV9_control treated mice		p=1 U=9	
Fig4d	Integrated time in response to formalin in the groups of AAV9_mutH3.1-treated <i>vs</i> sham operation	Non-parametric Mann-Whitney test	In the 1 <sup>st</sup> phase: p=0.166 U=3  In the 2 <sup>nd</sup> phase: p=0.166 U=3	6 AAV9_mutH3.1 treated and 3 sham-operated mice
Fig4d	Integrated time in response to formalin in the groups of control_AAV9-treated <i>vs</i> sham operation	Non-parametric Mann-Whitney test	In the 1 <sup>st</sup> phase: p=0.4 U=2  In the 2 <sup>nd</sup> phase: p=0.1 U=0	3 AAV9_control treated and 3 sham-operated mice
Fig4e	The overall influence of the treatment with the AAV9_mutH3.1 on body weight	Kruskal-Wallis ANOVA	p=0.32 df=3 $\chi^2=3.472$	7
Fig4e	The overall influence of the treatment with the control-AAV9 on body weight	Kruskal-Wallis ANOVA	p=0.141 df=3 $\chi^2=5.453$	5
Fig4e	The overall influence of sham operation on body weight -	Kruskal-Wallis ANOVA	p=0.975 df=3 $\chi^2=215$	4
Fig4e	Changes in body weight of AAV9_mutH3.1-treated <i>vs</i> sham operation between the corresponding days	Non-parametric Mann-Whitney test	day7: p=0.109 U=5; day14: p=0.927 U=13; day21: p=0.763 U=12	7 AAV9_mutH3.1-treated and 4 sham operated mice
Fig4e	Changes in body weight of AAV9_mutH3.1-treated <i>vs</i> AAV9_control treated mice between the corresponding days	Non-parametric Mann-Whitney test	day7: p=0.267 U=10; day14: p=0.755 U=15; day21: p=0.972 U=18	7 AAV9_mutH3.1-treated and 5 AAV9_control treated mice

## Supplementary Data S1.

The complete sequence of the designed construct with color codes corresponds to **Fig. 2c** in the main text. Bases in black represent segments without any annotated function.

ttcaggcaggtgctccaggttaattaaacattaataccccaccaaccatcccttaaaccccttacacttgctcagctaattacagcccgaggagaaggcgc  
cgtcccgccgctcacctgtggagtaacgcggtcagttagcagagccggggcggcggcgaggcggcggagcggggcacggggcgaaggcagcgc  
gcgactccgcggccgcgcgttcgttttatagggccgc  
gcacctctccgcctgcccccccccccccccccccccccccccccccccccccatgcgcacaaaataattaaaa  
ataaataaatacaaattgggggtggggggggggagatggggagagtgaagcagaacgtgggctcacctgaccatggtaatagcgatgactaatcg  
tagatgtactgccaagttagaaagtcccataaggcatgtactggcacaatgccaggcggcattaccgtattacgtcaatagggcgtacttggcata  
tgatacacttgtactgccaagtggcagttaccgttaactccaccattgacgtcaatggaaagtccctattggcttactattgacgtcaatggcgg  
ggtcgttggcggcagccaggcggccattaccgttaactgcaactttctatacaaaggtagggcctattccatgattccatattgcata  
tacgatacaaggcttagagagataattgaaattaatttactgtaaacacaaagatattgtacgtacgttagaaagtaataatttcttggtagt  
ttcagtttaaaattatgtttaaatggactatcatatgcttaccgttaacttggacttatttcgatttgcattatcatatcttggaaaggacgaaacaccgT  
GTCCTAAACAGACCCACAgtttagagctagaaatagcaagttaaataaggctgtccgttatcaactgaaaatggcaccgagtccgtcttttt  
tggcggccgagggcctattccatgattccatattgcatacgtacgttagggactatggacttatttgcattatcatatcttggaaaggacgaaacaccg  
tgcgttggcttatatatcttggaaaggacgaaacaccgGCCGCCGGTGGACTTGCAGgtttagagctagaaatagcaagttaaataagg  
tagtccgttatcaactgaaaatggcaccgagtccgtctttttggcggccgagggcctattccatgattccatattgcatacgtacgttagggactat  
tagagagataattgaaattaatttactgtaaacacaaagatattgtacgttagaaagtaataatttcttggtagttgcattttaaatta  
tgtttaaatggactatcatatgcttaccgttaacttggacttatttcgatttgcattatcatatcttggaaaggacgaaacaccgGGTGGCTAGCTGC  
TTGCAGCGtttagagctagaaatagcaagttaaataaggctgtccgttatcaactgaaaatggcaccgagtccgtc